Hierarchical diffusion, aging and multifractality

1997 J. Phys. A: Math. Gen. 30 1143

(http://iopscience.iop.org/0305-4470/30/4/016)

J. Phys. A: Math. Gen. **30** (1997) 1143–1160. Printed in the UK PII: S0305-4470(97)73561-3

Hierarchical diffusion, aging and multifractality

Hajime Yoshino†
Institute of Physics, University of Tsukuba, Tsukuba, Japan

Received 12 April 1996, in final form 18 October 1996

Abstract. We study toy aging processes in hierarchically decomposed phase spaces where the equilibrium probability distributions are multifractal. We found that the auto-correlation function, survival-return probability, shows crossover behaviour from a power law t^{-x} in the quasi-equilibrium regime ($t \ll t_w$) to another power law $t^{-\lambda}$ ($\lambda \geqslant x$) in the off-equilibrium regime ($t \gg t_w$) obeying a simple t/t_w scaling law. The exponents x and λ are related with the so-called *mass exponents* which characterize the multifractality.

1. Introduction

The *aging* processes, i.e. relaxational processes to approach the thermal equilibrium, are extremely slow in glassy systems like spin-glasses and one can observe remarkable *aging effects* in experiments [1, 2]. Among the various phenomenological descriptions of the aging effects are those by Sibani and Hoffman [3] who proposed a scenario based on the concept, *hierarchical diffusion* [4]. The latter concept has been implemented in many toy models [5–8], which we hereafter refer to as *hierarchical diffusion models*. The concept [10] is roughly as the following. First, one considers that the free-energy landscape consists of hierarchically nested valleys, which are usually described in terms of a certain *tree* structure. Then one introduces a relaxational dynamics in terms of a certain master equation which describes diffusion processes between different valleys driven by thermal hoppings over the barriers. Solving the master equation, one obtains the time evolution of the distribution of probabilities to find the system at different bottoms of valleys (or *leaves* of the trees).

In the present paper, we consider hierarchical diffusion in a class of trees which have the following two characteristics. First, we consider that the backbone structures of the trees have self-similarity as in many of the previously studied models. Secondly, we consider that the equilibrium probability distributions on the leaves are multifractal. The latter point is different from the previously studied models, whose equilibrium probability distributions are restricted to be uniform by their designs (see however [9]‡). We introduce the relaxational dynamics in terms of an exactly solvable master equation.

We study aging processes after rapid temperature quenches in our model. An aging process appears as the growth of sub-trees in which the probability distributions are quasi-equilibrium (multifractal) whereas on larger scales than such sub-trees the probability

† Present address: Institute for Solid State Physics, University of Tokyo, 7-22-1 Roppongi, Minato-ku, Tokyo, 106 Japan. E-mail address: yhajime@ginnan.issp.u-tokyo.ac.jp)

‡ Nemoto considered mimicking the dynamics of spin-glasses at low temperatures by an hierarchical diffusion model. He constructed random trees using information of the metastable states of the SK model, in which both the heights of the branch points and the statistical weights of the leaves have randomness. The present work is in part inspired by his work.

0305-4470/97/041143+18$19.50

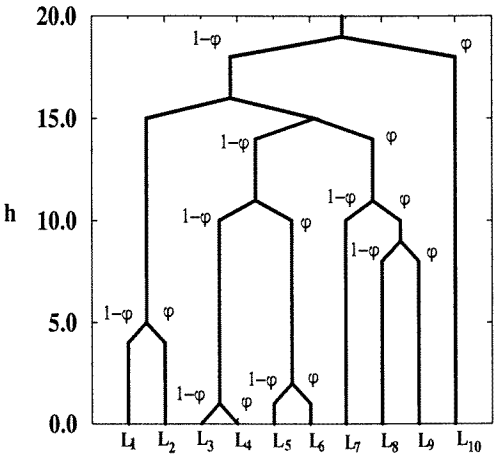

Figure 1. Hierarchical organization of *states*. This example is generated by a RBP explained in section 2.4.2 ($p_{\mathrm{branch}} = 0.10$, $\mathrm{d}b = 1.0$, $F(\psi) = \delta(\psi - 0.2)$, 20 MCS.) All the branches on the left side have weight $1 - \psi = 0.8$ while those on the right side have weight $\psi = 0.2$ as indicated in the figure.

distributions are still non-equilibrium (non-multifractal). As the result, a simple autocorrelation function, the survival-return probability, shows a characteristic crossover behaviour: it decays by a power law t^{-x} in the quasi-equilibrium regime ($t \ll t_{\mathrm{w}}$) but by another power law $t^{-\lambda}$ in the off-equilibrium regime ($t \gg t_{\mathrm{w}}$) and obeys a simple t/t_{w} scaling. The exponents x and λ turns out to be related with the so-called *mass* exponents which characterize the multifractal properties of the probability distributions.

The organization of this paper is the following. In section 2, we introduce our hierarchical diffusion model. In section 3, we analyse the aging effect in our model focusing on the scaling properties of an autocorrelation function. In section 4, we summarize this paper with some discussions.

2. The model

2.1. Construction of a tree

Let us consider a system of many *states* which have the following clustering property. Suppose that the system can be coarse-grained so that different *states* merge into fewer numbers of *states*. In figure 1, we show such a system represented as a tree. The magnitude of the resolution power increases downwards along the h-axis: the *states* (branches) are differentiated into more states (branches) as we raise the resolution power. We label the *states* differentiated with the maximum resolution power (the *leaves* on the baselines of the trees) as L_i ($i = 1 \ldots N$) where N is the number of such states.

For simplicity, we will only consider bifurcating trees: at every branch point we always have two branches stemming down. We will refer to the set of branches and branch points under a branch point, say A, as sub-tree A. We will refer one and the other side under a branch point A as side I and II of A and present them on the left and right side respectively in the figures.

We construct the partition function of the system at the equilibrium as follows. The coarse-grained states (branches) at the same resolution level are considered to be all

energetically degenerate with each other. However, the number of *microscopic* states they contain can vary, which means that the equilibrium local entropies and so the equilibrium statistical weights can vary as well. We consider that as a bifurcation takes place downwards along the h-axis (the direction to increase the resolution power), the equilibrium local entropy of a coarse-grained state is partitioned into those of two sub-states underneath. In order words, the partition function of sub-tree B is partitioned into those of side I and side II sub-trees under B with a certain partition ratio, say $1-\psi(B)$ and $\psi(B)$ $(0 \leqslant \psi \leqslant 1)$, respectively.

Let us denote the child of B (a branch point just below B) on side I as $C_I(B)$ and side II as $C_{II}(B)$. Then the ratio of the partition function of sub-tree $C_I(B)$ and $C_{II}(B)$ to that of B, which we denote as $\pi(\acute{B}, B)$, takes the following values,

$$\pi(\acute{B}, B) = \begin{cases} 1-\psi_B & \acute{B} = C_I(B) \\ \psi_B & \acute{B} = C_{II}(B). \end{cases} \tag{1}$$

It is useful to generalize the above argument as the following. Suppose that a sub-tree D is enclosed by a larger sub-tree B. Let us denote the *parent* of D (the branch point just above D) as D_1 and the *grand-parent* of D (the *parent* of D_1) as D_2 and so on. Suppose that B is the Kth *ancestor* of D, i.e. $D_K = B$. Then the ratio of the partition function of sub-tree D to that of sub-tree B, which we denote as $\pi(D, B)$, can be written as the product of π along the (unique) vertical *path* which connects D and B,

$$\pi(D, B) \equiv \pi(D, D_1)\pi(D_1, D_2)\ldots\pi(D_{K-1}, B). \tag{2}$$

For example, consider the set of leaves in a sub-tree B. Then $\pi(L_i, B)$ associated with such a leaf L_i can be interpreted as the *relative* statistical weight of the leaf among the set of leaves in sub-tree B. We denote the highest branch point as B_{top} and choose the partition function of the whole tree to be 1. Then the equilibrium statistical weight of a leaf L_i can be written as $\pi(L_i, B_{\text{top}})$.

Here we define some other terminologies for later uses. We denote the *ancestors* and *descendants*, which are the set of branch points above and below the branch point B, as $\mathcal{A}(B)$ and $\mathcal{D}(B)$ respectively. We denote the set of all branch points under sides I and II of B as $\mathcal{D}_I(B)$ and $\mathcal{D}_{II}(B)$ respectively. (Note that $\mathcal{D}_I(B) \cup \mathcal{D}_{II}(B) = \mathcal{D}(B)$.) We denote the *parent*, *grand-parent* and the Kth ancestor of B as B_1, B_2 and B_K respectively as we already did above. We denote the *lowest common ancestor* of B and $\acute{B}$, the branch point at the top of the smallest sub-tree which enclose both B and $\acute{B}$, as $A(B, \acute{B})$. For the convenience, we also introduce a hypothetical branch point B_{ceiling} whose height is $h_{B_{\text{ceiling}}} = \infty$ and set $\pi(B_{\text{top}}, B_{\text{ceiling}}) = 1$.

2.2. The master equation

We now introduce a stochastic dynamics of the temporal state in the hierarchically decomposed phase space. We consider that there is a thermally activated *excitation* associated with a branch point, say B, in the tree with which the temporal state can go from one to the other leaves in sub-tree B. The excitations associated with the branch points at higher h are considered to have higher activation energies to be excited. Thus, we now redefine the vertical h-axis as the scale of the activation energies of such excitations associated with the branch points.

We now introduce a simple exactly solvable dynamics which describes the stochastic jumps between the leaves, i.e. the states which are differentiable with the maximum resolution power. Hereafter we call the latter simply as *states*. Let us denote the probability

to find the temporal state of the system at a state L_i at time t as $p_i(t)$. The time-dependent distribution of the probability can be expressed in terms of a vector,

$$\boldsymbol{p}(t) = (p_1(t), p_2(t), \ldots, p_N(t)) \tag{3}$$

which should become equal to the equilibrium probability distribution in the limit $t \to \infty$. We denote the latter as $\boldsymbol{p}^{\mathrm{eq}} = (p_1^{\mathrm{eq}}, p_2^{\mathrm{eq}}, \ldots, p_N^{\mathrm{eq}})$ where

$$p_i^{\mathrm{eq}} \equiv \pi(L_i, B_{\mathrm{top}}). \tag{4}$$

Let us denote the transition probability to go from state L_j to L_i in a unit time as $\boldsymbol{W}_{ij}$. Then the master equation for the evolution of the probabilities can be written as

$$\frac{\mathrm{d}}{\mathrm{d}t}\boldsymbol{p}(t) = -\boldsymbol{\Gamma}\boldsymbol{p}(t) \tag{5}$$

with

$$-\boldsymbol{\Gamma}_{ij} = \boldsymbol{W}_{ij} - \delta_{ij}\sum_k \boldsymbol{W}_{kj}. \tag{6}$$

Note that the sum of the probability $\sum_{i=1}^{N} p_i(t)$ is always conserved.

We consider that the thermal jump process of the temporal state from a state (leaf) L to another state consists of two stages. In the first stage, the excitations associated with the branch points in $\mathcal{A}(L)$ (ancestors of L) are activated in a successive manner as the following. Suppose that the excitation associated with such a branch point B is activated. Then its parent B_1 get a chance to become active or not with the probability $\exp(-(h_{B_1} - h_B))$ and $1 - \exp(-(h_{B_1} - h_B))$ respectively. If B_1 becomes active, we repeat the same trial for B_2. Otherwise, the successive ignition of the excitations stop there at the level h_B. Thus, the probability that the first stage ends at B is

$$\begin{aligned} w(B \leftarrow L) &= \prod_{n=1}^{K} \exp(-(h_{A_n} - h_{A_{n-1}}))\left(1 - \exp(-(h_{B_1} - h_B))\right) \\ &= \exp(-h_B) - \exp(-h_{B_1}) \end{aligned} \tag{7}$$

where $A_0 = L$ and $A_K = B$.

The second stage is the *falling down* process from the height h_B to a leaf of sub-tree B. Reminding that the leaves $\acute{L} \in \mathcal{D}(B)$ have different relative statistical weights $\pi(\acute{L}, B)$, we expect that the probabilities to fall into the leaves depend on their amount of local entropies in such a way that those with larger amount of local entropies have more chances to *receive* the temporal state. So we simply choose the probability to fall down to a state (leaf) $\acute{L}$ as

$$w(\acute{L} \leftarrow B) = \pi(\acute{L}, B). \tag{8}$$

Combining the above two factors, we obtain the transition probability to go from L to $\acute{L}$ via B as

$$\begin{aligned} w(\acute{L}|B|L) &= w(\acute{L} \leftarrow B)w(B \leftarrow L) \\ &= \pi(\acute{L}, B)[\exp(-h_B) - \exp(-h_{B_1})]. \end{aligned} \tag{9}$$

Note, however, that such a process takes place only if both L and $\acute{L}$ belong to the sub-tree B.

The transition probability W_{ij} from L_j to L_i is the sum of the transition probabilities over A_n of $n = 0, 1, \ldots, M-1$ where $A_0 = A(L_i, L_j)$ (the lowest common ancestor of L_i and L_j) and $A_M = B_{\mathrm{ceiling}}$. Thus, the off-diagonal elements of the matrix $\boldsymbol{W}$ becomes

$$\boldsymbol{W}_{i\neq j} = \sum_{n=0}^{M-1} w(L_j|A_n|L_i) = \sum_{n=0}^{M-1}[\exp(-h_{A_n}) - \exp(-h_{A_{n+1}})]\pi(L_i, A_n) \tag{10}$$

Using (4) and (10), it can be checked that the detailed balance condition

$$\boldsymbol{W}_{ij} p_j^{\mathrm{eq}} = \boldsymbol{W}_{ji} p_i^{\mathrm{eq}} \tag{11}$$

is satisfied with this choice.

2.3. Solution of the master equation

We now solve the master equation (5). The formal solution can be written as

$$\boldsymbol{p}(t) = \exp(-\boldsymbol{\Gamma} t)\boldsymbol{p}(0) \tag{12}$$

where $\boldsymbol{p}(0)$ is the initial distribution at $t = 0$. The probability that the temporal state which initially stay at L_j reach L_i at time t is

$$\boldsymbol{G}_{ij}(t) = [\exp(-\boldsymbol{\Gamma} t)]_{ij}. \tag{13}$$

In order to calculate the propagator $\boldsymbol{G}$, it is convenient to introduce a new matrix $\tilde{\boldsymbol{\Gamma}}$ with which we can rewrite $\boldsymbol{\Gamma}$ as

$$\boldsymbol{\Gamma} \equiv (\boldsymbol{p}^{\mathrm{eq}})^{1/2} \tilde{\boldsymbol{\Gamma}} (\boldsymbol{p}^{\mathrm{eq}})^{-1/2} \tag{14}$$

where $\boldsymbol{p}^{\mathrm{eq}}$ is the vector of equilibrium statistical weights p_i^{eq} defined in (4). Note that $\tilde{\boldsymbol{\Gamma}}$ is a real symmetric matrix so that it has real eigenvalues.

We now look for the N eigenstates of $\tilde{\boldsymbol{\Gamma}}$ in a heuristic way. First of all, the *static* mode can be found easily as the following. The matrix $\boldsymbol{\Gamma}$ satisfies $\boldsymbol{\Gamma}\boldsymbol{p}^{\mathrm{eq}} = 0$ due to (6) and (11), from which we obtain $\tilde{\boldsymbol{\Gamma}}(\boldsymbol{p}^{\mathrm{eq}})^{1/2} = 0$. The last equation means that the vector $(\boldsymbol{p}^{\mathrm{eq}})^{1/2}$ is an eigenvector whose eigenvalue is 0, i.e. *static* mode. There are $N - 1$ other eigenstates (*dynamic modes*) left to be found.

We construct here a set of vectors which consists of vectors localized under the branch points. We may call this set of vectors an *umbrella set* because of the localized shape of the amplitudes. On a branch point B we define a vector

$$\hat{S}_i(B) = \pi^{1/2}(L_i, B) u(L_i, B) \tag{15}$$

where

$$u(\acute{B}, B) = \begin{cases} 1 & B = B_{\mathrm{ceiling}} \\ \sqrt{\dfrac{\psi_B}{1-\psi_B}} & B \neq B_{\mathrm{ceiling}} \ \acute{B} \in \mathcal{D}_{\mathrm{I}}(B) \\ -\sqrt{\dfrac{1-\psi_B}{\psi_B}} & B \neq B_{\mathrm{ceiling}} \ \acute{B} \in \mathcal{D}_{\mathrm{II}}(B) \\ 0 & \text{otherwise.} \end{cases} \tag{16}$$

Note that the vector $\hat{S}_i(B_{\mathrm{ceiling}})$ is identical to the eigenvector of the static mode we obtained above. It can be easily checked that the vectors are normalized and orthogonal,

$$\sum_i \hat{S}_i(B)\hat{S}_i(\acute{B}) = \delta_{B,\acute{B}}. \tag{17}$$

Since there are $N-1$ eigenvectors on $N-1$ branch points and one static mode, which are all linearly independent with each other, they together constitute a complete set of dimension N. As shown in appendix A, the vector $\hat{S}_i(B)$ actually turns out to be the correct eigenvectors of $\tilde{\boldsymbol{\Gamma}}$ which have the associated eigenvalues

$$\hat{z}(B) = \exp(-h_B). \tag{18}$$

Note that $\hat{z}(B_{\mathrm{ceiling}}) = 0$ (static mode) is endured since we have set $h_{B_{\mathrm{ceiling}}} = \infty$.

Now we rewrite some previously defined matrices in terms of the umbrella set. At first, $\tilde{\mathbf{\Gamma}}$ becomes

$$\tilde{\mathbf{\Gamma}}_{ij} = \sum_B \hat{S}_i(B)\hat{z}(B)\hat{S}_j(B). \tag{19}$$

Then using the last equation and (15) in (14), the matrix $\mathbf{\Gamma}_{ij}$ becomes

$$\begin{aligned}\mathbf{\Gamma}_{ij} &= (p_i^{\rm eq})^{1/2}\tilde{\mathbf{\Gamma}}_{ij}(p_j^{\rm eq})^{-1/2} \\ &= \sum_B \pi(L_i, B)u(L_i, B)u(L_j, B)\hat{z}(B).\end{aligned} \tag{20}$$

Finally, we also rewrite the propagator $\boldsymbol{G}$ in terms of the umbrella set. Using (13), (14) and (19) we obtain,

$$\begin{aligned}\boldsymbol{G}_{ij}(t) &= (p_i^{\rm eq})^{1/2}\sum_B\{\hat{S}_i(B)\exp(-\hat{z}(B)t)\hat{S}_j(B)\}(p_j^{\rm eq})^{-1/2} \\ &= \sum_B \pi(L_i, B)u(L_i, B)u(L_j, B)\exp(-\hat{z}(B)t).\end{aligned} \tag{21}$$

Using (15) and (16) and performing similar calculus shown in appendix A, we obtain the propagator in a more explicit form,

$$\boldsymbol{G}_{ij}(t) = \sum_{n=0}^{M-1}[\exp(-\hat{z}(A_{n+1})t) - \exp(-\hat{z}(A_n)t)]\pi(L_i, A_n) + \delta_{ij}\exp(-\hat{z}(A_0)t) \tag{22}$$

where we defined $A_0 = A(L_i, L_j)$ and $A_1, A_2, \ldots, A_{M-1}$, $A_M = B_{\rm ceiling}$.

2.4. Multifractality on self-similar trees

2.4.1. Mass exponents In this paper we consider self-similar trees on which the distributions of the equilibrium statistical weights have the following multifractal characteristics. Let us define the qth *moments* of the statistical weights [16] as,

$$M_q(h)\,{\rm d}h \equiv \overline{\sum_{\acute{B}\in\mathcal{D}(B)} \delta(h - (h_B - h_{\acute{B}}))\pi^q(\acute{B}, B)}\,{\rm d}h \tag{23}$$

where the over-line means the average over statistically independent sub-trees B. Suppose that a qth moment have the following scaling behaviour,

$$M_q(h)\,{\rm d}h \sim \exp(\tau(q)h)\,{\rm d}h, \tag{24}$$

where the exponent $\tau(q)$ is called as a *mass exponent* [16]. If $\tau(q)$ depends nonlinearly on q, the distribution is regarded as *multifractal*.

The geometrical self-similarity appears in the zeroth moment $M_0(h)$, which is just the number of leaves of a tree of height h. The mass exponent $\tau(0)$ is the fractal dimension of the tree and sometimes called a *silhouette* of the tree [8], which measures whether a given tree is *slender* or *fat*. A trivial exponent is $\tau(1)$ which is always zero because of the normalization condition of the statistical weights. Another exponent which turns out to be quite important is the mass exponent of the second moment $\tau(2)$. As we see later, the two exponents $\tau(0)$ and $\tau(2)$ are related with the dynamic exponents of the survival-return probability in the present model.

2.4.2. Randomly branching trees As an example of the trees which have the multifractal properties mentioned above, we construct here a specific class of random trees generated by the following randomly branching process (RBP). We use this specific example later when some demonstrations are necessary.

An RBP starts with a single *leaf*, which is regarded as the highest branch point $B_{\rm top}$ and two branches stemming down from it. In a single step, the length of the branches under the lowest (new) branch points get longer by one unit, say db so that the height (from the baseline of the tree) of all branch points and so that the height of the tree get larger by db. The branching at a leaf occurs with probability $p_{\rm branch}$ in a single step. When it takes place, the leaf becomes a new branch point and two new branches start from it. Each of such events occurs independently from each other. Repeating this procedure, we obtain a backbone structure of a tree.

Next we assign the *weights* on the tree. Consider a branch point B and its child (the branch points just below B) C_I on side I and C_{II} on side II. We determine the variable ψ_B and assign $\pi(C_I, B) = 1 - \psi_B$ and $\pi(C_{II}, B) = \psi_B$ to the branches on the side I and II of B. The variable ψ_B on each branch point is chosen randomly from the distribution

$$F(\psi)\,{\rm d}\psi \equiv \text{probability that } \psi_B \text{ lies between } \psi \text{ and } \psi + {\rm d}\psi. \tag{25}$$

We perform this procedure for the whole branch points.

Consider a tree which grows larger by the RBP. A natural consequence of the RBP is that the backbone structure possesses statistical self-similarities. On the other hand, the statistical weights on the leaves are successively partitioned further into more and more fine pieces by the RBP. It is well known that if such a process is repeated, one often finds very peculiar distribution of the weights: some set of pieces which have rather larger weights but negligibly smaller population compared with the *typical* ones which come to rapidly dominate the total sum of the statistical weights (the partition function of the whole tree) as the branching proceed further. This phenomena is called *curdling* [15] of multifractal objects.

As we show in appendix B, we actually obtain the scaling property of the form (24) in the case of the random trees generated by the RBP. The mass exponent is,

$$\tau(q) = {\rm d}b^{-1} \log \left[p_{\rm branch} \int_0^1 {\rm d}\psi\, F(\psi)\{\psi^q + (1-\psi)^q\} + (1 - p_{\rm branch}) \right]. \tag{26}$$

It can be seen that it is generally nonlinear with q. In figure 2 we show an example of $\tau(q)$ on random trees generated by a RBP. A special case when $\tau(q)$ becomes linear with q is when the following two conditions hold: $p_{\rm branch} = 1$ (deterministic branching) and $F(\psi) = \delta(\psi - \frac{1}{2})$ (always symmetric partition).

The real samples of such random trees can be generated numerically by the following Monte Carlo method. In one Monte Carlo step (MCS), the height of all branch points are raised by db. Simultaneously a pseudo-random number is generated for every leaf and if it is smaller than $p_{\rm branch}$, a bifurcation takes place: the leaf becomes a new branch point and two new branches start from it. Figure 1 is actually an example of such a random tree obtained by simulating the RBP of $p_{\rm branch} = 0.10$, ${\rm d}b = 1.0$ and $F(\psi) = \delta(\psi - 0.2)$ for 20 MCS.

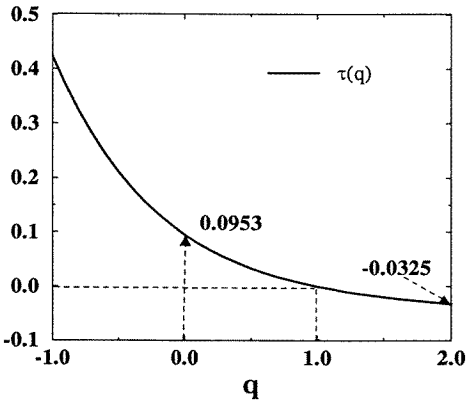

Figure 2. The nonlinear behaviour of the mass exponent $\tau(q)$ versus q: the curve is obtained using (26) for RBP of $p_{\text{branch}} = 0.10$, $\mathrm{d}b = 1.0$ and $F(\psi) = \delta(\psi - 0.2)$. The two important values of $\tau(q)$ at $q = 0$ and $q = 2$ are indicated by the arrows for later reference.

3. Aging effect

3.1. Growth of quasi-equilibrium domain

We now consider an aging process after rapid temperature quench from high temperature. For this purpose, we choose the initial configuration as,

$$\boldsymbol{p}(0) = \frac{1}{N}. \tag{27}$$

After waiting for t_{w} (waiting time), the probability distribution evolves up to,

$$\boldsymbol{p}(t_{\text{w}}) = \boldsymbol{G}(t_{\text{w}})\boldsymbol{p}(0) \tag{28}$$

which eventually become $\boldsymbol{p}^{\text{eq}}$ as $t_{\text{w}} \to \infty$. Note that the initial non-equilibrium distribution is not multifractal because it is uniform, while the final fully equilibrated distribution is multifractal. Hence, the aging process in the present context can be understood as the process to approach a multifractal distribution from a non-multifractal distribution.

In order to see how the system *ages*, it is convenient to define

$$r_i(t_{\text{w}}) \equiv p_i(t_{\text{w}})/p_i^{\text{eq}} = \frac{1}{N}\sum_B \exp(-\hat{z}(B)t_{\text{w}})\pi^{-1}(B, B_{\text{top}})\tilde{u}(L_i, B) \tag{29}$$

where we used (21) in (28) and defined

$$\tilde{u}(L_i, B) = u(L_i, B)\sum_{j\in\mathcal{D}(B)} u(L_j, B). \tag{30}$$

In figure 3 we show an example of $r_i(t_{\text{w}})$ calculated using the exact solution of the master equation solved on a real sample of random tree shown in figure 1. One can see that, as t_{w} increases, $r_i(t_{\text{w}})$ of different states come to join with each other successively and constitute groups, among each of which the values of $r_i(t_{\text{w}})$ are common. Note that as far as the transitions within such groups are concerned, the detailed balance (11) is fulfilled. Thus, we may call such a group of states a *quasi-equilibrium domain*.

In order to understand the growth mechanism of the *quasi-equilibrium domain* in a more formal way, let us introduce a characteristic height $h^{\text{eff}}(t_{\text{w}})$ which grows logarithmically with t_{w},

$$h^{\text{eff}}(t_{\text{w}}) \equiv \log(t_{\text{w}}). \tag{31}$$

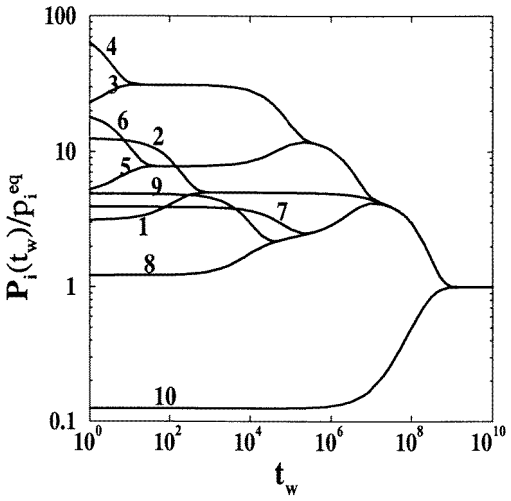

Figure 3. Growth of local equilibrium domain with increasing waiting time t_w: the plot of $r_i(t_w) \equiv p_i(t_w)/p_i^{eq}$ versus t_w on the random tree shown in figure 2.

Due to the factor $\exp(-\hat{z}(B)t_w) \simeq \exp(-\exp(h^{eff}(t_w) - h_B))$, the contributions from the branch points lower than $h^{eff}(t_w)$ in the r.h.s. of equation (29) are negligibly small, compared with those from the branch points higher than $h^{eff}(t_w)$. So it can be roughly approximated as

$$r_i(t_w) \simeq \sum_{h(B) \gg h^{eff}(t_w)} \exp(-\hat{z}(B)t_w)\pi^{-1}(B, B_{top})\tilde{u}(L_i, B). \tag{32}$$

Consider a pair of states L_i and L_j whose lowest common ancestor is $A(L_i, L_j)$. Suppose that after certain waiting time t_w^*, the characteristic height $h^{eff}(t_w^*)$ becomes larger than $h_{A(L_i,L_j)}$. Then from the definitions (30) and (16), all the terms that survive in the sum of (32) become the same for L_i and L_j. Consequently $r_i(t_w) = r_j(t_w)$ holds forever for $t_w \gg t_w^*$.

To summarize, the aging process of the present hierarchical model is understood as the growth of *aged* sub-trees or quasi-equilibrium domains. Here we mean by a quasi-equilibrium domain a sub-tree under a branch point lower than the characteristic height $h^{eff}(t_w)$, which grows logarithmically with t_w. The probability distributions inside an aged sub-tree is almost the same as that of a fully equilibrated one except for a common multiplicative factor. This is one of the most important consequence of *hierarchical diffusion* and actually found to be the case in the relaxational dynamics of microscopic spin-glass models [11].

The probability distribution inside an aged sub-tree is multifractal and possess the same scaling behaviours as that of the fully equilibrated one while on higher scale $h \gg h^{eff}(t_w)$, the system is still highly non-equilibrium or *young* in the sense that the probability distribution is not multifractal.

3.2. Survival-return probability

We now introduce one of the simplest auto-correlation functions as proof, that is the survival-return probability,

$$q(t+t_{\rm w},t_{\rm w}) \equiv \sum_i \boldsymbol{p}_i(t_{\rm w})\boldsymbol{G}(t)_{ii}. \tag{33}$$

It measures the probability that the system returns to the leaf where it stayed at time $t_{\rm w}$ after additional travelling of t.

Using (21), the autocorrelation function can be rewritten in terms of the umbrella set as

$$\begin{aligned} q(t_{\rm w},t+t_{\rm w}) &= \sum_i \boldsymbol{p}_i(t_{\rm w})\boldsymbol{G}(t)_{ii} \\ &= \sum_B \exp(-\hat{z}_B t)\sum_i p_i(t_{\rm w})\pi(L_i,B)u^2(L_i,B) \\ &= \int {\rm d}z\rho_{t_{\rm w}}(z)\exp(-zt) \end{aligned} \tag{34}$$

where we defined a kernel $\rho_{t_{\rm w}}(z)$ as

$$\rho_{t_{\rm w}}(z) \equiv \sum_B \delta(z-\hat{z}_B)\left\{\sum_i p_i(t_{\rm w})\pi(L_i,B)u^2(L_i,B)\right\}. \tag{35}$$

In the latter sections, we study the scaling behaviours of the survival-return probability in random trees generated by RBP focusing on the role played by the waiting time $t_{\rm w}$.

3.3. Two extreme cases

3.3.1. Zero waiting time. We consider at first a special case of zero-waiting time $t_{\rm w}=0$, which means that the system is in an extremely non-equilibrium condition at $t=0$. Since we have set the initial condition as (27), we obtain

$$\begin{aligned} \rho_0(z) &= \frac{1}{N}\sum_B \delta(z-\hat{z}(B)) \\ &= \frac{1}{N}\sum_B \delta(h-h_B))\,{\rm d}h, \end{aligned} \tag{36}$$

where we used (18) and defined a variable $h \equiv -\log(z)$.

Using (23) and (24), we obtain

$$\begin{aligned} \frac{1}{N}\sum_B \delta(h-h_B)\,{\rm d}h &= \frac{1}{N}\sum_{B\in\mathcal{D}(B_{\rm top})} \delta\left((h_{B_{\rm top}}-h)-(h_{B_{\rm top}}-h_B)\right)\pi^0(B,B_{\rm top})\,{\rm d}h \\ &\simeq \frac{1}{N}M_0(h_{B_{\rm top}}-h)\,{\rm d}h \simeq \exp\left(-\tau(0)h\right)\,{\rm d}h \\ &\simeq z^{s-1}\,{\rm d}z \end{aligned} \tag{37}$$

where $s=\tau(0)$ is the silhouette. In the last equation we used $N \simeq M_0(h_{B_{\rm top}})$ where $B_{\rm top}$ is the highest branch point. In the above equations, we approximated the sums by their mean values (23) assuming that the contributions of the deviations from this mean value vanish in the thermodynamics limit $N\to\infty$, i.e. *self-averaging*. This assumption is valid on trees generated by the RBP because quantities on sub-trees under different branch points at the same height are statistically independent from each other.

Then using (37), we obtain a power law decay in the off-equilibrium limit

$$q(0,t) = \int \mathrm{d}z \Omega(z) \exp(-zt) \sim t^{-\lambda} \tag{38}$$

where the exponent λ is equal to the fractal dimension or silhouette of the tree,

$$\lambda = s = \tau(0). \tag{39}$$

The above result is similar to those of the previously studied hierarchical diffusion models, which also yield power law decays whose exponents are related with the silhouette of the trees [5–8]. It is, however, not surprising because the distributions of the equilibrium probabilities in such models are uniform which is also the case for the present choice of the initial condition (27).

3.3.2. Infinite waiting time. The special case of infinite waiting time $t_w = \infty$ is also of interest. In this limit, the system is fully equilibrated or aged at $t = 0$. Using $p_i(\infty) = p_i^{\mathrm{eq}}$ and (4), we obtain

$$\rho_\infty(z) = \sum_B \delta(z - \hat{z}(B)) \left\{ \sum_i p_i^{\mathrm{eq}} \pi(L_i, B) u^2(L_i, B). \right\} \tag{40}$$

$$= \sum_B \delta(z - \hat{z}(B)) \pi(B, B_{\mathrm{top}}) \sum_i \pi^2(L_i, B) u^2(L_i, B)$$

$$= \sum_B \delta(z - \hat{z}(B)) \pi(B, B_{\mathrm{top}}) \Phi_B(z) \tag{41}$$

where we defined

$$\Phi_B(z) \equiv \delta(z - \hat{z}_B) \sum_{L_i \in \mathcal{D}(B)} \pi^2(L_i, B) u^2(L_i, B) \tag{42}$$

$$= \frac{\psi_B}{1 - \psi_B} \delta(z - \hat{z}_B) \sum_{L_i \in \mathcal{D}_I(B)} \pi^2(L_i, B) \frac{1 - \psi_B}{\psi_B} \delta(z - \hat{z}_B) \sum_{L_i \in \mathcal{D}_{II}(B)} \pi^2(L_i, B). \tag{43}$$

It is sufficient to consider the scaling property of the first term in the last equation. We can rewrite it as,

$$\delta(z - \hat{z}_B) \sum_{L_i \in \mathcal{D}_I(B)} \pi^2(L_i, B) \sim M_2(h) \sim z^{-\tau(2)} \tag{44}$$

where we wrote $h \equiv -\log(z)$. In the first equation, we evaluated the sum by the mean value (23) assuming *self-averaging* property and used (24). Thus, $\Phi_B(z)$ scales with z as $\Phi_B(z) \sim z^{-\tau(2)}$. In the same way we obtain,

$$\sum_B \delta(z - \hat{z}_B) \pi(B, B_{\mathrm{top}}) \, \mathrm{d}z \sim M_1(h_{B_{\mathrm{top}}} - h) \, \mathrm{d}h$$

$$\sim \mathrm{constant} \frac{\mathrm{d}z}{z} \tag{45}$$

where we wrote again $h = -\log(z)$ and used $\tau(1) = 0$. Combining above results we obtain

$$\rho_\infty(z) \, \mathrm{d}z \sim z^{-\tau(2)-1} \, \mathrm{d}z. \tag{46}$$

Using (46) in (34), we finally obtain another power law in the fully equilibrated limit,

$$q(t + \infty, \infty) \sim t^{-x} \tag{47}$$

where x is an exponent defined as,

$$x = -\tau(2). \tag{48}$$

Let us make some comments on the difference between the two dynamical exponents λ and x. Generally, the inequality $\lambda \geqslant x$ and equivalently $\tau(0) \geqslant -\tau(2)$ hold as long as $\tau(q)$ decreases monotonically with increasing q and concave downward. (Note that $\tau(1) = 0$ holds always as we mentioned before.) The latter conditions seem to be usually satisfied. This is certainly the case on the mass exponents of trees generated by the RBP whose formula is given in (26). The equality holds only when $p_{\text{branch}} = 1.0$ (deterministic branching) and $F(\psi) = \delta(\psi - 0.5)$ (always symmetric partition) so that the equilibrium probability distribution becomes the same as the initial non-equilibrium (non-multifractal) distribution.

3.4. Crossover behaviour: aging effect

Now we consider the case of *finite* waiting time, in which we expect some waiting time effects, i.e. crossover from quasi-equilibrium to off-equilibrium behaviour. It is now convenient to introduce another kernel $\tilde{\rho}(z, \acute{z})$ such that

$$\rho_{t_w}(z) \equiv \int \mathrm{d}\acute{z}\, \tilde{\rho}(z, \acute{z}) \exp(-\acute{z} t_w). \tag{49}$$

Then the autocorrelation function (34) can be rewritten as

$$q(t + t_w, t_w) = \int \mathrm{d}z \int \mathrm{d}\acute{z}\, \tilde{\rho}(z, \acute{z}) \exp(-zt) \exp(-\acute{z} t_w). \tag{50}$$

From (35), (28) and (21) we obtain the explicit form of the kernel $\tilde{\rho}(z, \acute{z})$ as

$$\tilde{\rho}(z, \acute{z}) = \frac{1}{N} \sum_B \sum_{\acute{B}} \delta(z - \hat{z}(B)) \delta(\acute{z} - \hat{z}(\acute{B})) \times \left\{ \sum_i \pi(L_i, B) \pi(L_i, \acute{B}) u^2(L_i, B) u(L_i, \acute{B}) \sum_j u(L_i, \acute{B}) \right\}. \tag{51}$$

The scaling form of $\tilde{\rho}(z, \acute{z})$ is studied in appendix C. Here we read the result,

$$\tilde{\rho}(z, \acute{z})\, \mathrm{d}z\, \mathrm{d}\acute{z} \sim \begin{cases} z^{-\tau(2)} \dfrac{\mathrm{d}z}{z} \dfrac{\mathrm{d}\acute{z}}{\acute{z}} & (z > \acute{z}) \\ \left(\dfrac{z}{\acute{z}}\right)^{\tau(0)} \acute{z}^{-\tau(2)} \dfrac{\mathrm{d}z}{z} \dfrac{\mathrm{d}\acute{z}}{\acute{z}} & (z < \acute{z}). \end{cases} \tag{52}$$

Using (52) in (50), we finally obtain

$$q(t + t_w, t_w) \sim t^{\tau(2)} \tilde{q}_1(t/t_w) + t^{-\tau(0)} t_w^{\tau(0)+\tau(2)} \tilde{q}_2(t/t_w) \tag{53}$$

where we defined

$$\tilde{q}_1(s) \equiv C_1 \int \mathrm{d}y\, y^{-\tau(2)-1} \exp(-y) \int^{y/s} \mathrm{d}\acute{y}\, \acute{y}^{-1} \exp(-\acute{y})$$
$$\tilde{q}_2(s) \equiv C_2 \int \mathrm{d}y\, y^{\tau(0)-1} \exp(-y) \int_{y/s} \mathrm{d}\acute{y}\, \acute{y}^{-(\tau(0)+\tau(2))-1} \exp(-\acute{y}) \tag{54}$$

where C_1 and C_2 are numerical prefactors.

From the above results, we find that the autocorrelation function obeys the following simple t/t_w type scaling,

$$q(t + t_w, t_w) \sim t^{-x} \tilde{q}(t/t_w) \tag{55}$$

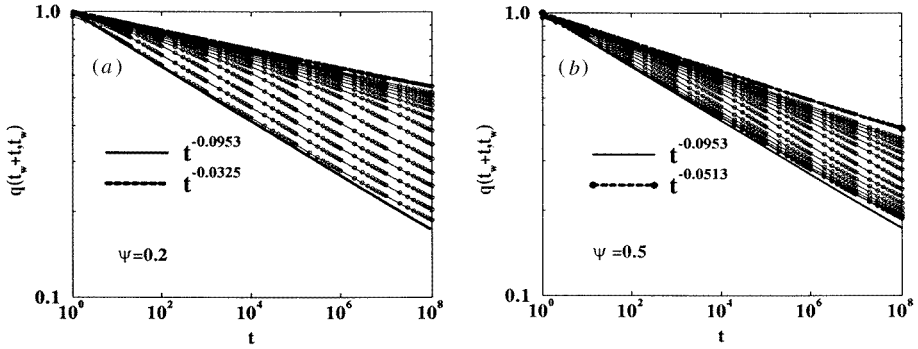

Figure 4. The crossover behaviour of $q(t_w + t, t_w)$ at different t_w on two specific kinds of random trees (a) and (b) (see text). The t_w varies as $t_w = 0, 10, 10^2, \ldots, 10^{14}, \infty$ from the lowest to the top curve.

where the scaling function $\tilde{q}(y)$ behaves as

$$\tilde{q}(y) \sim \begin{cases} \text{constant} & (y \ll 1) \\ y^{x-\lambda} & (y \gg 1) \end{cases} \tag{56}$$

with $x = -\tau(2)$ and $\lambda = \tau(0)$.

From the above scaling form, it can be seen that the autocorrelation function crossovers from quasi-equilibrium behaviour t^{-x} to off-equilibrium behaviour $t^{-\lambda}$ at around $t \sim t_w$. This crossover behaviour appears due to the growth of the quasi-equilibrium domain in which the probability distribution is multifractal while on larger scale, it is still non-equilibrium (non-multifractal). The inequality of the two exponents $\lambda \geqslant x$ means that the off-equilibrium decay is *faster* than the quasi-equilibrium decay, which is intuitively satisfactory.

We show in figure 4 some examples of the crossover behaviour of the autocorrelation function, which was obtained using the exact solutions of the master equation on real samples of random trees. The random trees are generated by the Monte Carlo method which simulate the RBP of (a) $p_{\text{branch}} = 0.10$, d$b = 1.0$ and $F(\psi) = \delta(\psi - 0.2)$ and (b) $p_{\text{branch}} = 0.10$, d$b = 1.0$ and $F(\psi) = \delta(\psi - 0.5)$. The random average was took over 10^3 different realizations of such trees generated by 50 Monte Carlo steps. The predicted power law $t^{-\lambda}$ and t^{-x} with (a) $\lambda = \tau(0) = 0.0953\ldots$ and $x = -\tau(2) = 0.0325\ldots$ (see figure 2) and (b) $\lambda = \tau(0) = 0.0953\ldots$ and $x = -\tau(2) = 0.0513\ldots$ which are obtained from (26), are also included in the figure. The curvatures of the curves at lower values of q are due to the finite size effects. In figure 5 we show the scaling plot of the data shown in figure 4(a). The curves of different t_w are plotted against t/t_w and shifted vertically so as to converge to a master curve. One can well see that the data are consistent with the predicted scaling laws (55) and (56).

4. Discussion

We have studied aging effects in a simple exactly solvable model of hierarchical diffusion. We considered the case that equilibrium probability distribution has multifractality. A specific way to generate such trees by randomly branching processes (RBP) are introduced for demonstrations. Aging processes after temperature quenches appear as the growth of aged sub-trees in which the probability distribution is in quasi-equilibrium and multifractal. In the thermodynamics limit, the height of the tree becomes infinite and the true equilibrium

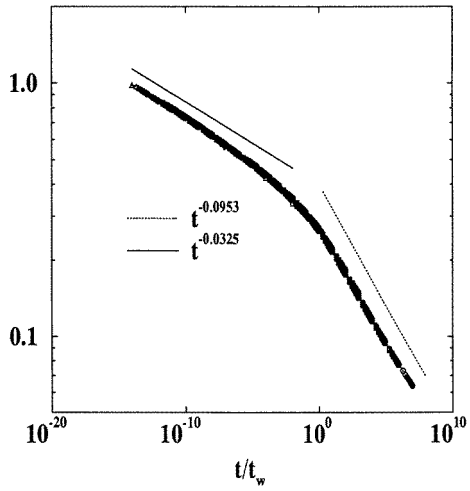

Figure 5. The t/t_w scaling plot of $q(t_w + t, t_w)$: the data of of different t_w presented in figure 4(a) except $t_w = 0$ and ∞, are used in this plot. The vertical scale is arbitrary.

cannot be attained in any large but finite t_w. Consequently, the waiting time dependence persists for the whole range of t_w except for $t_w = \infty$, i.e. the ergodicity is weakly broken [12]. We found that these properties are clearly reflected in the survival-return probability and brings about the characteristic crossover from quasi-equilibrium behaviour to off-equilibrium behaviour.

Let us make some comments on the robustness of the scaling properties of the autocorrelation function we obtained in our exactly solvable model. Note that there are other possible choices of the transition matrix other than our present choice, which describe hierarchical diffusions and endures the detailed balance condition (11). For instance, one may define another transition matrix by replacing $\pi(L_i, A_n)$ in (10) by $\pi(L_j, A_n)^{-1}$. One can also construct transition matrices considering that transitions between a pair of leaves occur only over their lowest common ancestor. We investigated the solutions of the master equations with these alternative transition matrices on random trees generated by the RBP by numerical diagonalizing the transition matricies. Interestingly enough, we found that the scaling behaviours of the autocorrelation function appears essentially the same as that of the exactly solvable one presented in this paper and one only needs some renormalization of the global unit of time. This fact implies that the scaling properties are robust to some extent against minor changes of the model.

It is interesting to note that the crossover behaviour from *quasi-equilibrium* behaviour ($t \ll t_w$) to *off-equilibrium* behaviour ($t \gg t_w$) obtained in the present toy model, is very similar to that observed in the relaxational dynamics of some microscopic models of random systems such as the three-dimensional spin-glass model [13] and (1+1)-dimensional directed polymer in random media [14]. In the latter models, the autocorrelation functions obey t/t_w scaling law with two power law decays t^{-x} at the quasi-equilibrium regime and $t^{-\lambda}$ at the off-equilibrium regime, which is what we found in the present phenomenological toy model. Thus, it is tempting to speculate that our present toy model will provide a clue to understanding the link between phenomenological pictures based on hierarchical diffusion and the glassy dynamics of realistic systems†.

† In the case of SK model, which is a mean-field spin-glass model, it is known [19] that the participation ratio

Acknowledgments

The author would like to sincerely thank Professor Takayama for valuable discussions and critical reading of the manuscript. The communications with Professor Bouchaud and Professor Sibani are gratefully acknowledged. He would also like to thank Professor Nemoto, Professor Arimitsu and Dr Hukusima for stimulating discussions and valuable comments. This work was supported by a Grant-in-Aid for Scientific Research from the Ministry of Education, Science and Culture, Japan. The author was supported by Fellowships of the Japan Society for the Promotion of Science for Japanese Junior Scientists.

Appendix A. The umbrella set

In this appendix we show that the umbrella set defined in (15), (16) and (18) are the true eigenstates of the matrix $\tilde{\mathbf{\Gamma}}$ defined in (14). We prove this by checking if the umbrella set correctly reproduces the original transition matrix defined in (10).

Using (15) and (18) in (20) we obtain

$$\begin{aligned}-\mathbf{\Gamma}_{i\neq j} &= -\sum_B \pi(L_i, B)u(L_i, B)\hat{z}(B)u(L_j, B) \\ &= \pi(L_i, A(L_i, L_j))\exp(-h_{A(L_i,L_j)}) \\ &\quad - \sum_{B\in\mathcal{A}(A(L_i,L_j))} \pi(L_i, B)\exp(-h_B)u^2(L_j, B) \\ &= \pi(L_i, A_0)\exp(-h_{A_0}) - \sum_{n=1}^{M}\pi(L_i, A_n)\exp(-h_{A_n})u^2(L_j, A_n)\end{aligned}$$

where we defined $A_0 = A(L_i, L_j)$ and $A_1, A_2, \ldots, A_{M-2}$, $A_{M-1} = B_{\text{top}}$ and $A_M = B_{\text{ceiling}}$.

We further rewrite the r.h.s. of the last equation as follows. The factor $u(L_j, A_n)$ in the last equation can be replaced by $u(A_{n-1}, A_n)$ due to the definition (16). And the factor $\pi(L_i, A_n)$ can be decomposed as $\pi(L_i, A_{n-1})\pi(A_{n-1}, A_n)$. Then we can use the identity $\pi(A_{n-1}, A_n)u^2(A_{n-1}, A_n) = 1 - \pi(A_{n-1}, A_n)$, which follows from (16) and (1). Then we obtain

$$\begin{aligned}\text{r.h.s.} &= \pi(L_i, A_0)\exp(-h_{A_0}) - \sum_{n=1}^{M}\pi(L_i, A_{n-1})(1-\pi(A_{n-1}, A_n))\exp(-h_{A_n}) \\ &= \sum_{n=0}^{M-1}[\exp(-h_{A_n}) - \exp(-h_{A_{n+1}})]\pi(L_i, A_n) \qquad (57)\end{aligned}$$

where we used $h_{A_M} = h_{B_{\text{ceiling}}} = \infty$ in the last equation. Then using the relation (6), we see that the off-diagonal elements of the transition probability $\boldsymbol{W}_{i\neq j}$ defined in equation (10) is correctly reproduced by the umbrella set.

$\sum_\alpha W_\alpha^2$ where W_α is the equilibrium statistical weight of a pure state α, is non-zero. The latter means that the total statistical weight is dominated by only a few pure states. Contrarily, in the case of random trees generated by RBP, the participation ratio goes to zero as the height of the tree h becomes infinitely high because $\tau(2)$ is negative. Thus in the case of RBP trees, the survival-return probability goes to zero in the limit $t \to \infty$ even after the limit $t_{\text{w}} \to \infty$ is reached, while it might be non-zero in the case of SK model. I thank J P Bouchaud for pointing this out [18].

Next we check if the matrix $\mathbf{\Gamma}$, written in terms of the umbrella set, properly conserves the total probability. Taking the sum over i of both sides of (20) we obtain

$$\sum_i \mathbf{\Gamma}_{ij} = \sum_B \left(\sum_i \pi(L_i, B) u(L_i, B) \right) \hat{z}(B) u(L_j, B) = 0. \tag{58}$$

The last equation is derived from the following. For $B = B_{\text{ceiling}}$, the contribution is zero since $\hat{z}(B_{\text{ceiling}}) = 0$. And for $B \neq B_{\text{ceiling}}$, one finds again zero contributions using (15),

$$\begin{aligned}\sum_i \pi(L_i, B) u(L_i, B) &= \sqrt{\frac{\psi_B}{1-\psi_B}} \sum_{L_i \in \mathcal{D}_I(B)} \pi(L_i, B) - \sqrt{\frac{1-\psi_B}{\psi_B}} \sum_{L_i \in \mathcal{D}_{II}(B)} \pi(L_i, B) \\ &= \sqrt{\frac{\psi_B}{1-\psi_B}} (1-\psi_B) - \sqrt{\frac{1-\psi_B}{\psi_B}} \psi_B = 0.\end{aligned}$$

Thus we obtain the last equation of (58).

Appendix B. Mass exponents on random trees

In this appendix we study the scaling property of the qth moment of the probability distribution on the random trees generated by the randomly branching process (RBP) and derive the formula (26).

Let us denote the probability that the qth moment $M_q(h)$ of a random tree of size $h = m\,\mathrm{d}b$ takes value x as $\omega_q(m, x)$. Considering that larger trees can be constructed by smaller sub-trees, we obtain the following recursion relation for $\omega_q(m, x)$,

$$\begin{aligned}\omega_q(m+1, x) = p_{\text{branch}} \int \mathrm{d}y_1\, \mathrm{d}y_2 \int_0^1 \mathrm{d}\psi\; F(\psi) \omega_q(m, y_1) \omega_q(m, y_2) \\ \times \delta(\psi^q y_1 + (1-\psi)^q y_2 - x) + (1 - p_{\text{branch}}) \omega_q(m, x).\end{aligned} \tag{59}$$

In order to solve this integral equation, it is convenient to introduce a generating function defined as

$$Z_q(u, m) \equiv \int \mathrm{d}x \exp(ux) \omega_q(m, x). \tag{60}$$

The expectation value of the qth moment can be obtained as

$$M_q(h) \simeq \langle x \rangle_{q,m} \equiv \int \mathrm{d}x\, x \omega_q(m, x) = \frac{\partial}{\partial u} Z_q(u, m) \bigg|_{u=0}. \tag{61}$$

Multiplying $\exp(ux)$ on both sides of (59) and integrating over x, we obtain the recursion relation for $Z_q(u, M)$

$$Z_q(u, m+1) = p_{\text{branch}} \int_0^1 \mathrm{d}\psi\, F(\psi) Z_q(u\psi^q, m) Z_q(u(1-\psi)^q, m) + (1 - p_{\text{branch}}) Z_q(u, m). \tag{62}$$

Then we obtain the recursion relation for $\langle x \rangle_{q,m}$,

$$\langle x \rangle_{q,M+1} = \left[p_{\text{branch}} \int_0^1 \mathrm{d}\psi\, F(\psi) \{\psi^q + (1-\psi)^q\} + (1 - p_{\text{branch}}) \right] \langle x \rangle_{q,M}. \tag{63}$$

Solving the last equation with $\langle x \rangle_{q,1} = 1$, we obtain

$$M_q(h) \sim \langle x \rangle_{q,M} = \exp(\tau(q) h) \tag{64}$$

where the mass exponent $\tau(q)$ is obtained as

$$\tau(q) = \mathrm{d}b^{-1} \log\left[p_{\mathrm{branch}} \int_0^1 \mathrm{d}\psi \; F(\psi)\{\psi^q + (1-\psi)^q\} + (1 - p_{\mathrm{branch}}) \right]. \tag{65}$$

In order to further investigate the multifractal properties, it is convenient to introduce the *exponent of singularity* α defined as

$$\pi(B, \acute{B}) \equiv \exp[-\alpha(B, \acute{B})(h_B - h_{\acute{B}})]. \tag{66}$$

Then one can obtain the distribution of α or $f(\alpha)$ spectrum using the well known procedure [16] and discuss *curdling*. However, we do not discuss it here [17].

Appendix C. Scaling form of the kernel

In this appendix we study the scaling property of the kernel $\tilde{\rho}(z, \acute{z})$ with respect to z and $\acute{z}$. Its explicit form (51) is

$$\tilde{\rho}(z, \acute{z}) = \frac{1}{N} \sum_B \sum_{\acute{B}} \delta(z - \hat{z}(B)) \times \delta(\acute{z} - \hat{z}(\acute{B}))\left\{ \sum_i \pi(L_i, B)\pi(L_i, \acute{B})u^2(L_i, B)u(L_i, \acute{B}) \sum_j u(L_j, \acute{B}) \right\}. \tag{67}$$

Note that, from the definitions (16), the factor $u^2(L_i, B)u(L_i, \acute{B})$ is non-zero only when the leaf L_i is under both B and $\acute{B}$.

At first we consider the case $z > \acute{z}$. In this case, the terms which survive in the sum (67) are those in which $\acute{B}$ is an ancestor of B and B is an ancestor of L_i. Let us introduce $h \equiv -\log(z)$ and $\acute{h} \equiv -\log(\acute{z})$. Then we obtain

$$\begin{aligned}
\tilde{\rho}(z, \acute{z})\,\mathrm{d}z\,\mathrm{d}\acute{z}\,(z > \acute{z}) &= \frac{1}{N} \sum_{\acute{B} \in \mathcal{D}(B_{\mathrm{top}})} \delta(\acute{z} - \hat{z}(\acute{B}))\pi^0(\acute{B}, B_{\mathrm{top}}) \\
&\times \sum_{Lj \in \mathcal{D}(\acute{B})} \delta(\acute{z} - \hat{z}(B))\pi^0(L_j, \acute{B})u(L_j, \acute{B}) \\
&\times \sum_{B \in \mathcal{D}(\acute{B})} \delta(z - \hat{z}(B))\delta(\acute{z} - \hat{z}(\acute{B}))\pi^1(B, \acute{B})u(B, \acute{B}) \\
&\times \sum_{L_i \in \mathcal{D}(B)} \delta(z - \hat{z}(B))\pi^2(L_i, B)u^2(L_i, B)\,\mathrm{d}z\,\mathrm{d}\acute{z} \\
&\sim \frac{1}{N} M_0(h_{B_{\mathrm{top}}} - \acute{h}) M_0(\acute{h}) M_1(\acute{h} - h) M_2(h)\,\mathrm{d}h\,\mathrm{d}\acute{h} \\
&\sim z^{-\tau(2)} \frac{\mathrm{d}z}{z} \frac{\mathrm{d}\acute{z}}{\acute{z}}
\end{aligned} \tag{68}$$

where we evaluated the sums by their mean values (23), assuming *self-averaging* property, and used (26) and $N \simeq M_0(h_{B_{\mathrm{top}}})$.

The other case $z < \acute{z}$ can be analysed in the same way. Considering that the terms which survive in the sum (67) are those in which B is an ancestor of $\acute{B}$ and $\acute{B}$ is an ancestor of L_i, we obtain

$$\tilde{\rho}(z, \acute{z})\,\mathrm{d}z\,\mathrm{d}\acute{z}\,(z < \acute{z}) = \frac{1}{N} \sum_{B \in \mathcal{D}(B_{\mathrm{top}})} \delta(z - \hat{z}(B))\pi^0(B, B_{\mathrm{top}})$$

$$\times \sum_{\acute{B}\in\mathcal{D}(B)} \delta(z-\hat{z}(B))\delta(\acute{z}-\hat{z}(\acute{B}))\pi^1(\acute{B},B)u^2(\acute{B},B)$$
$$\times \sum_{L_i\in\mathcal{D}(\acute{B})} \delta(\acute{z}-\hat{z}(B))\pi^2(L_i,\acute{B})u(L_i,\acute{B})$$
$$\times \sum_{L_j\in\mathcal{D}(\acute{B})} \delta(z-\hat{z}(B))\pi^0(L_i,\acute{B})u(L_i,\acute{B})\,\mathrm{d}z\,\mathrm{d}\acute{z}$$
$$\sim \frac{1}{N}M_0(h_{B_{\mathrm{top}}}-h)M_1(h-\acute{h})M_2(\acute{h})M_0(\acute{h})\,\mathrm{d}h\,\mathrm{d}\acute{h}$$
$$\sim \left(\frac{z}{\acute{z}}\right)^{\tau(0)}\acute{z}^{-\tau(2)}\frac{\mathrm{d}z}{z}\frac{\mathrm{d}\acute{z}}{\acute{z}} \tag{69}$$

where we used again $N \simeq M_0(h_{B_{\mathrm{top}}})$. Combining the above results, we obtain (52).

References

[1] Vincent E, Hamman J and Ocio M 1992 *Recent Progress in Random Magnets* (Singapore: World Scientific)
[2] Struik L C E 1978 *Physical Aging in Amorphous Polymers and Other Materials* (New York: Elsevier)
[3] Sibani P and Hoffmann K H 1989 *Phys. Rev. Lett.* **63** 2853
Sibani P and Hoffmann K H 1990 *Z. Phys.* B **80** 429
[4] Hoffmann K H and Sibani P 1988 *Phys. Rev.* A **38** 4261
[5] Huberman B A and Kerszberg M 1985 *J. Phys. A: Math. Gen.* **18** L331
[6] Shreckenberg M 1985 *Z. Phys.* B **60** 483
[7] Ogielski A T and Stein D L 1985 *Phys. Rev. Lett.* **55** 1634
[8] Bachas C P and Huberman B A 1987 *J. Phys. A: Math. Gen.* **20** 4995
[9] Nemoto K 1988 *Cooperative Dynamics in Complex Physical Systems* ed H Takayama (Berlin: Springer)
[10] Palmer R G 1982 *Adv. In. Phys.* **31** 669
Palmer R G 1987 *Heidelberg Colloquium on Glassy Dynamics (Lecture Notes in Physics)* vol 275, ed J L van Hemmen and I Morgenstern (Berlin: Springer)
[11] Sibani P and Schriver P 1994 *Phys. Rev.* B **49** 6667
See also Sibani P, Schön J C, Salamon P and Anderson J O 1993 *Europhys. Lett.* **22** 479
[12] Bouchaud J P 1992 *J. Physique* **2** 1705
[13] Rieger H 1993 *J. Phys. A: Math. Gen.* **26** L615
Rieger H 1995 *Annual Reviews of Computational Physics* vol 2, ed D Stauffer (Singapore: World Scientific)
[14] Yoshino H 1996 *J. Phys. A: Math. Gen.* **29** 1421
[15] Mandelbrot B B 1982 *The Fractal Geometry of Nature* (San Francisco, CA: Freeman)
[16] Feder J 1988 *Fractals* (New York: Plenum)
[17] Yoshino H 1996 *PhD Thesis* University of Tsukuba
[18] Bouchaud J P Private communication
[19] Mézart M, Parisi G, Sourlas N, Toulouse G and Virasoro M 1984 *Phys. Rev. Lett.* **52** 1156
Mézart M, Parisi G, Sourlas N, Toulouse G and Virasoro M 1984 *J. Physique* **45** 843